Front. Optoelectron. 2020, 13(4): 360–370
https://doi.org/10.1007/s12200-020-1094-z

RESEARCH ARTICLE

Attenuation correction technique for fluorescence analysis of biological tissues with significantly different optical properties

Tatiana A. SAVELIEVA (✉)[1,2], Marina N. KURYANOVA[2], Ekaterina V. AKHLYUSTINA[2], Kirill G. LINKOV[1], Gennady A. MEEROVICH[1,2], Victor B. LOSCHENOV[1,2]

1 Prokhorov General Physics Institute of the Russian Academy of Sciences, Moscow 119991, Russia
2 National Research Nuclear University MEPhI, Moscow115409, Russia

© Higher Education Press 2020

Abstract During intraoperative fluorescence navigation to remove various neoplasms and during pharmacokinetic studies of photosensitizers in laboratory animals, in many cases, the ratio of photosensitizer accumulation in the tumor and normal tissue can reach ⩾10-fold, which inevitably changes their optical properties. At the same time, the tumor formation process causes various metabolic and structural changes at cellular and tissue levels, which lead to changes in optical properties. A hardware–software complex for the spectral–fluorescence studies of the content of fluorochromes in biological tissues with significantly different optical properties was developed, and it was tested on optical phantoms with various concentrations of photosensitizers, absorbers, and scatterers. To correct the influence of optical properties on the photosensitizer concentration analysis by fluorescence spectroscopy, we propose the spectrum-processing algorithm, which combines empirical and theory-based approaches.

Keywords fluorescence, spectroscopy, scattering, absorption, attenuation correction, optical phantoms

1 Introduction

The study on the pharmacokinetics and biodistribution of pharmaceutical agents is based on the assessment of their concentration in organs, tissues, and biological body fluids at specific points in time after administration. As a rule, such studies are performed in a wide range of administered doses of the agent. The content of the agent considerably varies in different organs and at different points in time. One of the most important requirements for such studies is a wide dynamic range of the measurement method, which must be at least three orders of magnitude.

Currently, the most promising approach for studying the pharmacokinetics and biodistribution of drugs with pronounced fluorescence properties is to use spectral–fluorescence techniques [1–3]. They are widely used to assess the level and selectivity of photosensitizer (PS) uptake in biological tissues for photodynamic therapy and fluorescence diagnostics. However, this method has various limitations, which are determined by the variability of the optical properties of the studied biological tissues and the high range of PS concentration in the tissue. During intraoperative fluorescence navigation and pharmacokinetic studies, in many cases, the ratio of PS accumulation in a tumor and normal tissue can reach ⩾10-fold, which inevitably changes their optical properties. At the same time, the tumor formation process causes various metabolic and structural changes at cellular and tissue levels, which also changes optical properties. A change in the optical properties of tissue depending on the wavelength affects both the excitation and fluorescence spectra of the studied PSs. In addition, changes in fluorescence intensity owing to changes in the fluorophore concentration cannot be distinguished from changes in the signal arising from changes in absorption and scattering without further analysis.

Thus, the task of eliminating the influence of optical properties on the method of analyzing the concentration of PS by fluorescence spectroscopy, as well as its analysis in the extended dynamic range, is very important. This problem has not been solved in a complex, but there are studies devoted to the solution of individual problems [4–

Received September 1, 2020; accepted October 1, 2020

E-mails: savelevat@gmail.com, tasavelyeva1@mephi.ru

6]. Currently available correction techniques fall into three broad categories: empirical techniques, measurement method-based techniques, and theory-based techniques [4]. Empirical attenuation correction techniques use reflectance information to subtract or divide fluorescence signal from the reflectance signal [7,8]; spatially resolved reflectance, assuming the concentration of an exogenous fluorophore, can be recovered by determining the fluorescence–reflectance ratio at a specific distance [9], or taking a ratio of fluorescence intensities at two emission wavelengths can be used to correct for changes in blood volume and oxygenation [10]. Measurement method-based techniques use nontrivial approaches for signal registration such as confocal detection, single-fiber detection with a fiber radius of < 100 μm, using polarized excitation light, and measuring the fraction of fluorescence and reflectance that retains polarization. This group of methods has a clear limitation in the area of tissue sample analysis. The information obtained from such small volume or depth can be non-relevant for the whole picture of metabolic changes and fluorophore concentration in the vicinity of this volume. Theory-based attenuation correction techniques use approximations to the energy transfer equation, i.e., modified Beer–Lambert law, Kubelka–Munk theory, and diffusion theory or Monte Carlo simulation techniques to eliminate the absorption and scattering effect on fluorescence signal. In this study, we combine empirical and theory-based techniques and use hardware capabilities. On the hardware level, it is necessary to take into account that the dynamic range of the spectrum analyzer is mainly determined by the characteristics of the matrix photodetector. At high levels of incident light on the cell of matrix photodetector, this cell and adjacent cells may undergo charge saturation; at low levels, the signal associated with the incident light may be hardly distinguishable against the background of hardware noise of the device (first of all, the noise of the matrix photodetector). Therefore, the dynamic range of known devices does not exceed two orders of magnitude. This can lead to the distortion of the shape of the spectra and to the dependence of their intensity on the content of PS in the studied biological tissue, which prevents the study of metabolic (biochemical) transformations of the PS, its pharmacokinetics, and biodistribution. One of the objectives of this study is to expand the dynamic range of a spectrum analyzer for pharmacokinetic and biodistribution studies.

The advantage of our approach to achieve a more accurate analysis of PS concentration is the use of the combination of hardware and software techniques. To eliminate the influence of significantly different optical properties on the signal at the hardware level, we propose the automatic real-time expansion of the dynamic range. At the software level, we correct the influence of different optical properties by determining the concentration of tissue components responsible for absorption and light scattering and extrapolating these data to the spectral range of fluorescence recording.

2 Materials and methods

2.1 Spectroscopic setup

The spectroscopic setup for recording the spectra of diffuse reflection and fluorescence is shown in Fig. 1 as a block diagram of the device with main components.

The spectroscopic equipment used for this study includes a laser, a polychromator, a fiber-optic probe (containing illuminating fibers that deliver excitation radiation to the biological tissue and receiving optical fibers for delivering fluorescence radiation from the biological tissue to the polychromator input), and a matrix

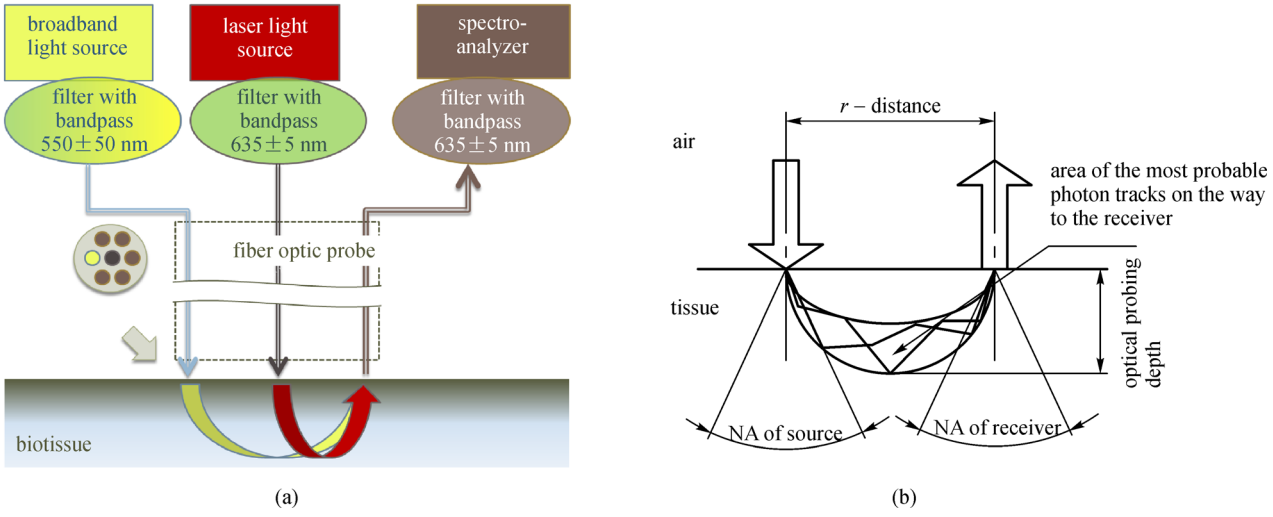


Fig. 1 (a) Block diagram of a spectral analyzer for the simultaneous recording of fluorescence and diffuse reflection spectra with a filter system for recording fluorescence of photosensitizers in the near-infrared range. (b) Scheme of signal formation in the fiber-optic probe

photodetector at the polychromator output. The signal recording system from each of the cells of the photodetector, proportional to its charge, includes an analog-to-digital converter (ADC), a block of buffer memory, and a computer (PC) [1]. In the spectral–fluorescence study, light from the laser output is introduced into the optical fiber probe.

For fluorescence measurements, a standard fiber probe, consisting of one central delivery fiber (for laser light), one peripheral delivery fiber (for white light), and five peripheral collecting metal-coated quartz fibers with the core diameter of 200 μm, was used. The fiber spacing was 250 μm (center-to-center) with a total diameter of the probe tip of 1.8 mm. The delivery fiber was coupled to a He–Ne laser (632.8 nm) with a 10-mW output power measured at the probe tip. The collecting fibers were coupled to a spectrometer LESA-01-BIOSPEC (JSC BIOSPEC, Russia) with a "cut-off" filter inserted at the entrance for suppressing the scattered laser light.

After coming out of the distal end of the illuminating fiber, this light irradiates biological tissue containing PS and initiates fluorescence of its molecules. The receiving optical fibers of the fiber-optic probe deliver fluorescence light from the biological tissue to the input of the polychromator, where the spectral decomposition of this light occurs, after which the light falls on the photodetector. The signal from the output of the photodetector enters ADC and the buffer memory unit. PC uses digital data coming from the output of the buffer memory, corresponding to the intensity of the signal from each cell of the photodetector, and cell numbers of the photodetector, for which a certain wavelength is set according to the calibration results, to form a spectral curve (intensity vs. wavelength), which is displayed on the computer screen. For the analysis of diffusely reflected radiation, an illumination fiber is used to deliver broadband radiation to the tissues, and a series of peripheral fibers of the optical fiber probe are used to deliver light, which is diffusely reflected by tissue, to the spectrometer.

To expand the dynamic range of intensity of registered signals, the following approach is proposed. During the spectral signal registration, the maximum and minimum values of the spectral density are automatically monitored. If these values were outside the specified range, the algorithm for automatically adjusting the exposure of the photodetector is initiated. This approach is described in more detail in our previous work [10].

2.2 Optical phantoms

To develop an algorithm for correcting the effect of optical properties on fluorescence signal, the following strategy was proposed. The experimental dependence of the fluorescence signal on the concentration of absorbing and light-scattering components measured from optical phantoms with significantly different optical properties were used after approximation to obtain the functional dependence of real PS concentration on fluorescence signal.

To physically model the scattering properties of biological tissues, solutions of fat emulsions are usually used. Polystyrene spheres are another classical material that is used to simulate the scattering properties of biological tissues [11]. Previously, we have already used this approach to model multilayered optical phantoms [12]. However, in this study, phantoms with fat emulsion were sufficient because we analyzed multiply scattered light, which made it possible to neglect differences in the scattering anisotropy factor for particles of a given size and to rely in the modeling on the correspondence of reduced scattering coefficient.

The limits of using the linear dependence of the scattering properties of fat emulsion, Intralipid solution on volume concentration, were investigated [13–15]. The absorption coefficient of fat emulsions in the visible spectrum at wavelengths exceeding 550 nm is negligible [16]. Thus, fat emulsions are the correct and convenient physical model of the scattering properties of biological media.

To simulate the scattering properties of biological media, an aqueous solution of lipofundin MCT/LST 20% was used, the optical properties of which are shown in Table 1 for a number of concentrations used. In Tables 1 and 2, the next parameters are listed: μ'_s is a reduced scattering coefficient equal to $\mu_s(1-g)$, where μ_s is scattering coefficient calculated as value reciprocal of the photon mean free path between scattering events, g is scattering anisotropy factor calculated as average cosine of scattering angle, and μ_a is absorption coefficient calculated as value reciprocal to photon mean free path to absorption event. To model absorption, an erythrocyte mass solution was used,

Table 1 Content of fat emulsion in optical phantoms and the corresponding values of the scattering coefficient in three spectral ranges in accordance with Ref. [3]

parameter	value				
fat emulsion concentration/%	0.5	1	2	4	8
μ'_s (550 nm)/cm^{-1}	7.5	15	30	60	120
μ'_s (632 nm)/cm^{-1}	6.5	13	26	52	104
μ'_s (700 nm)/cm^{-1}	5.5	11	22	44	88

Table 2 Blood content in optical phantoms and the corresponding values of the absorption coefficient in two spectral ranges in accordance with Ref. [17]

parameter	value			
blood content in tissues (% or mL/100 g)	1	2	4	8
Hb in tissue/(mmol·L^{-1})	0.024	0.048	0.096	0.192
HbO_2 μ_a (550 nm)/cm^{-1}	2.235	4.47	8.94	17.88
Hb μ_a (550 nm)/cm^{-1}	2.775	5.55	11.1	22.2
HbO_2 μ_a (632 nm)/cm^{-1}	0.032	0.064	0.128	0.256
Hb μ_a (632 nm)/cm^{-1}	0.267	0.534	1.068	2.136
HbO_2 μ_a (700 nm)/cm^{-1}	0.015	0.03	0.06	0.12
Hb μ_a (700 nm)/cm^{-1}	0.093	0.186	0.372	0.744

the optical properties of which are shown in Table 2 for a series of concentrations used. Protoporphyrin IX (PpIX) (for concentrations from 0 to 10 mg/L) was used as a fluorophore.

An array of optical phantoms was made, which contained a fat emulsion (as a scattering agent in a series of concentrations of 0.5%, 1%, 2%, and 8%), hemoglobin (Hb) (as an absorber in a series of concentrations corresponding to the blood content of 0%, 1%, and 4% and 0%, 1%, 2%, 4%, and 8% (by taking into account hematocrit 40%)), and PS (in the concentrations of 0, 1, 5, and 10 mg/L).

The phantoms were poured into 5-mL Eppendorf tubes. Trial measurements of the studied signals were performed through the Eppendorf wall and by immersion in the sample liquid. A decrease in the accuracy of the analysis using the first approach was shown; therefore, preference was given to measurements performed in contact with a liquid.

In Table 2, attention should be paid to the difference in the absorption coefficient depending on the degree of oxygenation and wavelength. As has already been mentioned, the average absorption coefficient decreases by an order of magnitude when moving from the neighborhood of 550 nm to the neighborhood of 632 nm and by another order of magnitude when passing through the near-infrared boundary. This property of hemoglobin absorption spectrum forms the so-called biological transparency window. However, attention should also be paid to the unevenness of these changes for hemoglobin in oxygenated and free forms. In the yellow–green region of the spectrum, despite the considerably different spectral shape of these forms of hemoglobin, their average absorption coefficients are very similar (the absorption of deoxyhemoglobin is only 25% higher than that of oxyform). At 632 nm, the absorption coefficient of desoxyhemoglobin exceeds the absorption coefficient of oxyform by almost an order of magnitude (8.3 times higher). In the region of 700 nm, this ratio slightly decreases and reaches the value of 6.2; however, it is still sufficiently large to talk about the need to take into account the effect of hemoglobin oxygenation on the fluorescence signal we recorded (just in the range of 700 nm). Thus, in this study, the concentration and degree of hemoglobin oxygenation in the region of 500–600 nm were analyzed.

2.3 Spectrum-processing algorithms

To develop the most effective algorithm of spectrum processing to correct fluorescence attenuation by scattering and absorption, a comparison of several approximations of experimental dependencies of fluorescence on optical properties was made. First, the ratio techniques were utilized. Specifically, the ratio of the areas under fluorescence spectrum around the peak and diffuse-reflected laser signal is obtained. We call it the fluorescence index. The fluorescence index provides a comprehensive account of absorption and scattering at the excitation wavelength and extrapolates their influence from the excitation wavelength to the fluorescence recording wavelength. However, there are at least two weak points in this approach. First, the optical properties at 632 and 700 nm, as shown above for the scatterer and absorber, are significantly different. Second, the ratio does not take into account the nature of attenuation of light in the tissue, which is usually described theoretically by an exponential law. An important advantage of the fluorescence index is its computational ease.

The fluorescence index for different concentrations can be used to determine the concentration of PS after spectrometer calibration. The calibration procedure consists of measuring the index value for a number of optical phantoms with known concentrations of the PS.

The aim of this work was to reduce the variation of the parameter characterizing the fluorescence of the PS for different concentrations of the absorber and scatterer in comparison with the fluorescence index.

For this purpose, various variants of approximating the dependence of signal at the fluorescence wavelength on the scatterer concentration were considered as well as the

possibility of using these approximations to take into account the effect of scattering on the fluorescence signal.

The first linear approximation was considered. Considering that linear regression coefficients depend on the concentration of the PS, the generalized dependence can be represented as

$$S([\mathrm{ps}],[\mathrm{il}])_{705} = (A([\mathrm{ps}]) \cdot [\mathrm{il}] + B([\mathrm{ps}])) / (C \cdot \mathrm{Hb}_{\mathrm{total}} - D), \quad (1)$$

$$A([\mathrm{ps}]) = a \cdot [\mathrm{ps}] + a_0,\ B([\mathrm{ps}]) = b \cdot [\mathrm{ps}] + b_0, \quad (2)$$

$$S([\mathrm{ps}],[\mathrm{il}])_{705} = ([\mathrm{ps}] \cdot (a \cdot [\mathrm{il}] + b) + a_0 \cdot [\mathrm{il}] + b_0) / (C \cdot \mathrm{Hb}_{\mathrm{total}} - D), \quad (3)$$

where [ps] is PS concentration, [il] is fat emulsion concentration, $\mathrm{Hb}_{\mathrm{total}}$ is total hemoglobin concentration, and A, B, C, D, a, a_0, b, and b_0 are fitting parameters.

The desired concentration of the PS is calculated as

$$[\mathrm{ps}] = (S([\mathrm{ps}],[\mathrm{il}])_{705} \cdot (C \cdot \mathrm{Hb}_{\mathrm{total}} - D) - a_0 \cdot [\mathrm{il}] - b_0) / (a \cdot [\mathrm{il}] + b). \quad (4)$$

The final equation for calculating the concentration of the PS was obtained in the form

$$[\mathrm{ps}] = (S([\mathrm{ps}],[\mathrm{il}])_{705} \cdot (3.6208\mathrm{Hb}_{\mathrm{total}} + 0.8529) + 0.0704[\mathrm{il}] - 1.0166)/(0.8882[\mathrm{il}] + 0.2867). \quad (5)$$

The next step for refining the experimentally described dependencies of fluorescence on the scatterer concentration is the approximation by a power function. This dependence is empirical and does not take into account the whole complex of factors of interaction of light with tissue; however, it is closer to the obtained dependencies than linear dependence and at the same time is advantageous for its computational simplicity.

The power law coefficients also depend on the concentration of the PS. In this case, the generalized dependence can be represented as

$$S([\mathrm{ps}],[\mathrm{il}])_{705} = C([\mathrm{ps}]) \cdot [\mathrm{il}]^{D([\mathrm{ps}]) - B \cdot \mathrm{Hb}_{\mathrm{total}}}. \quad (6)$$

After taking the logarithm of both sides of the equation and expanding the logarithm of the concentration of the PS into a Taylor series by taking two main terms, we obtain the dependence:

$$[\mathrm{ps}] = (\ln(S([\mathrm{ps}],[\mathrm{il}])_{705}) + 0.16 + (1.9481\mathrm{Hb}_{\mathrm{total}} - 0.3816) \cdot \ln[\mathrm{il}]) / (1.17 + 0.0626\ln[\mathrm{il}]). \quad (7)$$

The modified Beer–Lambert law describes the attenuation of radiation in strongly scattering absorbing media and takes into account an increase in the path of photons in the tissue owing to the effect of multiple scattering [18]:

$$A = \ln(I_0/I) = B \cdot \mu_a \cdot d + G, \quad (8)$$

where A is coefficient of light attenuation by a medium, which takes into account the effects of absorption and multiple scattering; B is factor of the average path length of a photon in tissue along the path from the source to the receiver at a given distance between them (d), depending on the coefficients of absorption, scattering, and scattering phase function; and G is factor that depends on the geometry of measurements and the scattering coefficient and does not depend on the absorption of light by the medium.

Let us imagine the molecules of a PS as a type of internally distributed source of fluorescence radiation in the tissue. In this case, the dependence of fluorescence signal reaching the receiving fiber on the concentration of the absorber and scatterer can be described as follows:

$$S([\mathrm{ps}],[\mathrm{il}])_{705} = C \cdot \mathrm{e}^{B \cdot (\mu_a(\mathrm{Hb}) + \mu_a(\mathrm{HbO_2})) + G}, \quad (9)$$

where $\mu_a(\mathrm{Hb}) = 2.303\varepsilon_{\mathrm{Hb}} \cdot [\mathrm{Hb}]/M$, $\mu_a(\mathrm{HbO_2}) = 2.303\ \varepsilon_{\mathrm{HbO_2}} \cdot [\mathrm{HbO_2}]/M$. [Hb] and [$\mathrm{HbO_2}$] are concentration of free and oxygenated hemoglobin, measured in g/L; $\varepsilon_{\mathrm{Hb}}$ and $\varepsilon_{\mathrm{HbO_2}}$ are molar extinction coefficient of free and oxygenated hemoglobin, measured in L/(mol·cm); and M is molar mass of hemoglobin equal to 66500 g/mol. G depends in some way on μ_s', e.g., linearly, $G = g \cdot \mu_s' + g_0$.

Considering all parameters, the dependence will take the form

$$S([\mathrm{ps}],[\mathrm{il}])_{705} = C \cdot \mathrm{e}^{B \cdot 2.303 \cdot [\mathrm{Hb_{total}}] \cdot (\varepsilon_{\mathrm{HbO_2}} \cdot (\mathrm{SO_2}) + \varepsilon_{\mathrm{Hb}} \cdot (1 - \mathrm{SO_2})) + g \cdot \mu_s' + g_0}, \quad (10)$$

$$[\mathrm{ps}] = \frac{S([\mathrm{ps}],[\mathrm{il}])_{705}}{\mathrm{e}^{B \cdot 2.303 \cdot [\mathrm{Hb_{total}}] \cdot (\varepsilon_{\mathrm{HbO_2}} \cdot (\mathrm{SO_2}) + \varepsilon_{\mathrm{Hb}} \cdot (1 - \mathrm{SO_2})) + g \cdot \mu_s' + g_0}}. \quad (11)$$

When recalculating the concentrations of absorbing and scattering components used in the experiment into the indicated optical parameters, the data shown in Tables 1 and 2 were used.

An approximation based on the Beer–Lambert law modified for multiple scattering and the approximate diffusion theory of radiation transfer was also proposed. The dependence was proposed as close as possible to the form of the solution of the diffusion approximation and compensated for the disadvantage of the modified Beer–Lambert law:

$$S([\mathrm{ps}],[\mathrm{il}])_{705} = C\cdot(\mu_a(\mathrm{total})+\mu_s')\cdot e^{B\cdot\sqrt{\mu_a(\mathrm{total})(\mu_a(\mathrm{total})+\mu_s')}+g\cdot\mu_s'+g_0}. \quad (12)$$

Hence, the concentration of the PS is

$$[\mathrm{ps}] = \frac{S([\mathrm{ps}],[\mathrm{il}])_{705}}{(\mu_a(\mathrm{total})+\mu_s')\cdot e^{B\cdot\sqrt{\mu_a(\mathrm{total})(\mu_a(\mathrm{total})+\mu_s')}+g\cdot\mu_s'+g_0}}. \quad (13)$$

3 Results and discussion

3.1 Investigation of the influence of exposure time on the calculated spectral characteristics

The dependence of diffusely reflected laser radiation and fluorescence intensity on the concentration of fat emulsion and PS are shown in Fig. 2.

In Figs. 2(a) and 2(b), an increase in the recorded signal (both diffusely reflected laser and fluorescence) is observed with an increase in the scatterer concentration. This is explained by the fact that the more scattering events that light undergoes, the higher is the probability that some of it will return back to the receiver. However, this growth is not constant, and the dependence tends to gradually reach a plateau. This can be explained by the geometry of the experiment. In our case, the signal is recorded not from the entire surface of the tissue but at a certain point at which the receiving fiber is located. The relative position of the illuminator and receiver affects the form of considered dependencies. With an increase in the concentration of fat emulsion, diffuse scattered photons are concentrated in the area closest to the light source, without penetrating deep into the tissue. They pass a smaller path in the tissue and do not have time to excite the same number of fluorophore molecules as in the case of a less scattering solution. This can lead to a decrease in the fluorescence index in strongly scattering solutions.

The dependence of fluorescence index on the concentration of fat emulsion and exposure time is shown in Fig. 3.

For different values of exposure time, we observe a negligible variation in the values of fluorescence index in the region of high concentrations of fat emulsion. This suggests the possibility of automatic exposure control during measurements without significant influence on such calculated parameter as fluorescence index. However, the absolute value of light scattering must be taken into account when calculating the fluorophore concentration because the calculated fluorescence index decreases with an increase in light scattering.

3.2 Investigation of the effect of absorption and scattering on the accuracy of determining the concentration of a photosensitizer from its fluorescence spectrum

Below are the results of measurements of the diffuse reflectance (DR) signal at the wavelengths of the laser and fluorescence radiation, as well as their ratio (fluorescence index), as a first approximation by taking into account the effect of absorption and scattering on the fluorescence signal.

Figures 4(a) and 4(b) show the effect of an increase in the fluorescence index in weakly scattering solutions owing to the limited cuvette size. For the high concentration of fat emulsion, we can see an increase in fluorescence index. This can be explained by the different growth rates of the dependence of laser signal and fluorescence on the scatterer concentration (Figs. 4(c) and 4(d)). The diffusively reflected laser signal tends to plateau faster than the fluorescence signal. The source of laser radiation is limited by the aperture of the illuminating fiber, and the source of fluorescence radiation is distributed in the volume of tissue, and the fluorescence process itself is

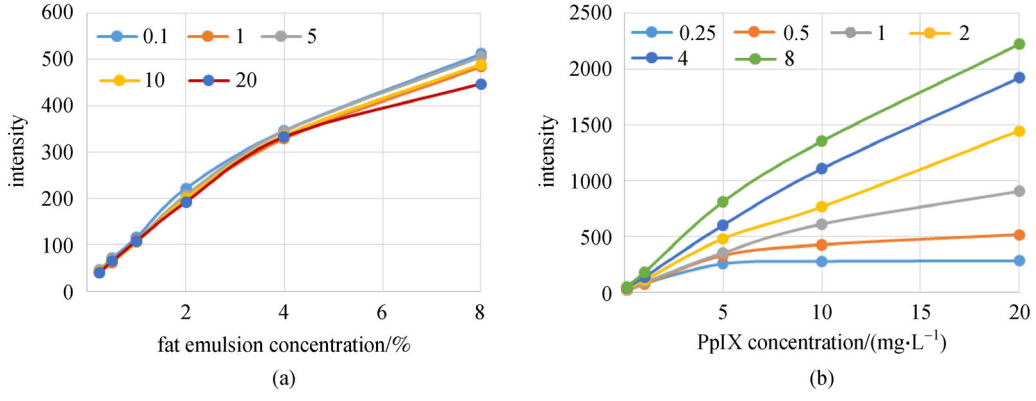


Fig. 2 (a) Dependence of diffusely reflected laser radiation on the concentration of fat emulsion for different fluorophore concentrations, marked with different colors. (b) Dependence of fluorescence intensity on the fluorophore concentration for different concentrations of fat emulsion, marked in different colors

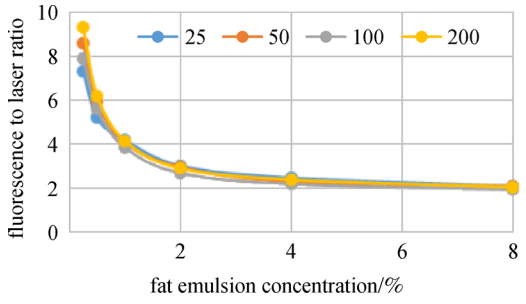


Fig. 3 Dependence of fluorescence index on the concentration of fat emulsion for different exposure values (in ms) for 1 mg/L of PpIX (without hemoglobin)

isotropic. Thus, fluorescence is better scattered by the medium than by the exciting laser light.

In this study, we considered these quality criteria for the parameter describing the concentration of fluorescence as its variation depending on the concentration of the scatterer and on the concentration of hemoglobin. Our goal was to minimize these criteria.

For a given PS concentration of 1 mg/L, the variation in the fluorescence index depending on scattering was 12% and that on the blood content was 13%. With an increase in the concentration of the PS to 10 mg/L, the variation of the fluorescence index significantly increases and reaches 44% of the variation depending on scattering. The variation depending on the blood content remains at the level of 12%.

To reduce the considered variations, we proposed several options for approximating the dependence of the fluorescence signal on the concentration of the scatterer and absorber.

The first considered approximation was linear according to Eq. (5) in Section 2. Figure 5 shows the results of correcting the fluorescence signal using a linear approximation.

As we can see, the result of reconstructing fluorescence information using linear approximation is unsatisfactory.

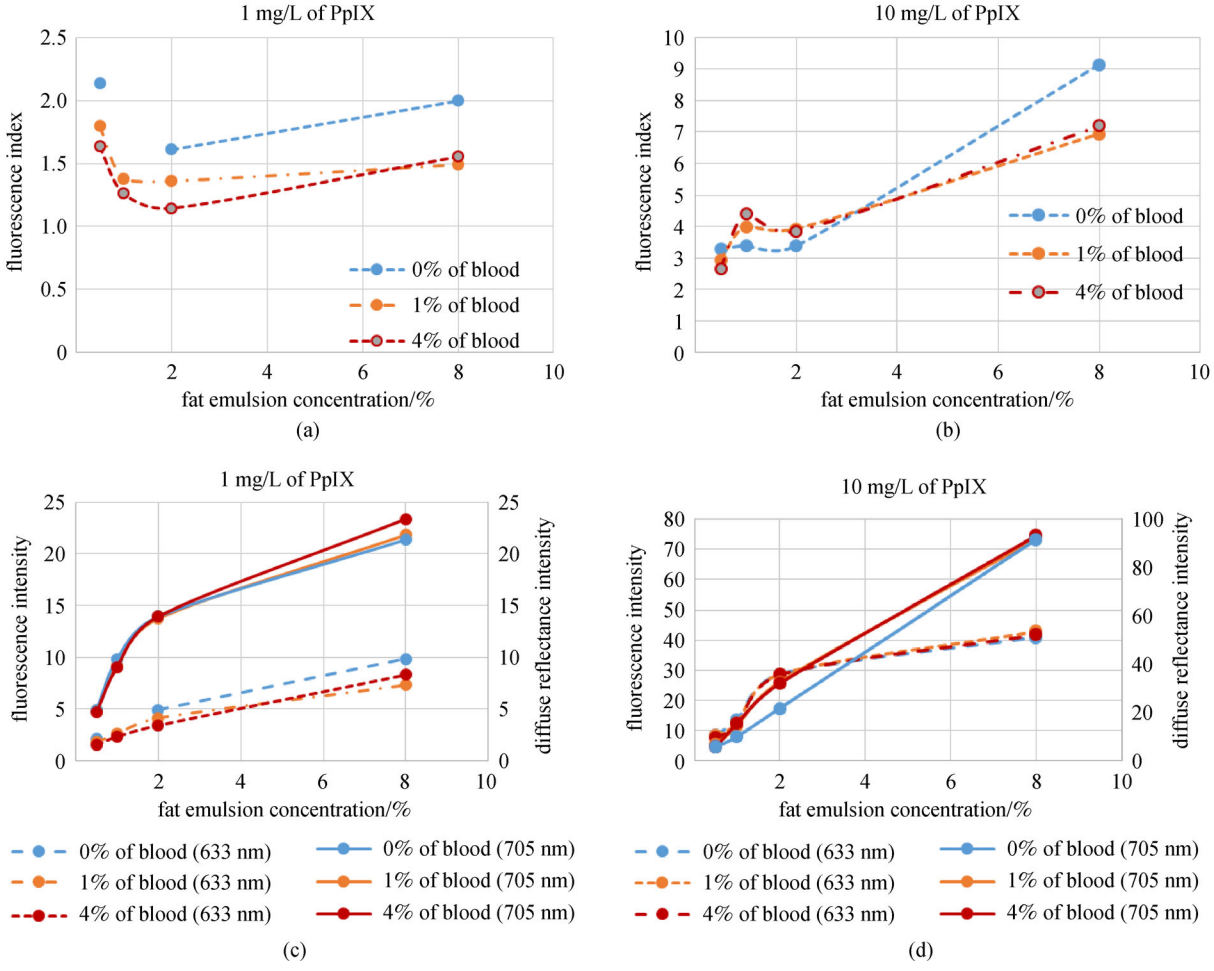


Fig. 4 Effect of the concentration of the scatterer (along the *x*-axis) and absorber (graphs are marked in different colors) on the fluorescence index for (a) 1 mg/L of PpIX and (b) 10 mg/L of PpIX and initial fluorescence and diffuse reflection dependencies for (c) 1 mg/L of PpIX and (d) 10 mg/L of PpIX

Though, on average, the variation of the parameter decreased from 28% to 14%, this was owing to a significant reduction in the calculation error for the PpIX concentration of 10 mg/L, whereas for 1 mg/L, the average variation, on the contrary, increased from 12% to 16%. Thus, we abandoned this computationally simple correction method in favor of those that more accurately accounted for the nature of dependences obtained in the experiment.

The power law approximation showed considerably better results (see Fig. 6). The average variation was 10.6%. At the same time, the variation for 1 mg/L decreased to 11.6% and to 9.6% for 10 mg/L.

The use of the Beer–Lambert law, modified by taking into account multiple scattering, did not lead to a decrease in the variation of the parameter under study because this dependence was strictly curved downward compared with the observed experimental dependences (Fig. 7). To compensate for this difference, we will perform an approximation by taking into account the multiple scattering of the Beer–Lambert law and the diffuse approximation of the radiation transport theory (Eq. (12)).

According to Eq. (13), we obtained the average variation equal to 16.3%.

By summarizing the results of studying various approximations, we concluded that the power law approximation is advantageous for our measuring probe configuration (Table 3).

The power law approximation is optimal for a given configuration of the fiber-optic sample, and it can be used to calculate the concentration of the PS at known concentrations of the scatterer and absorber with the least variation. We can extract the information about scattering and hemoglobin absorption from DR spectra in the spectral region from 500 to 625 nm according to the algorithm that we proposed earlier in Ref. [19].

There are many possibilities of using the proposed approach, e.g., in the field of fluorescence intraoperative navigation. In the case of using this approach when removing intracranial tumors, we observed a significant change in optical properties with a change in the degree of tissue malignancy [20]. The main contribution to the

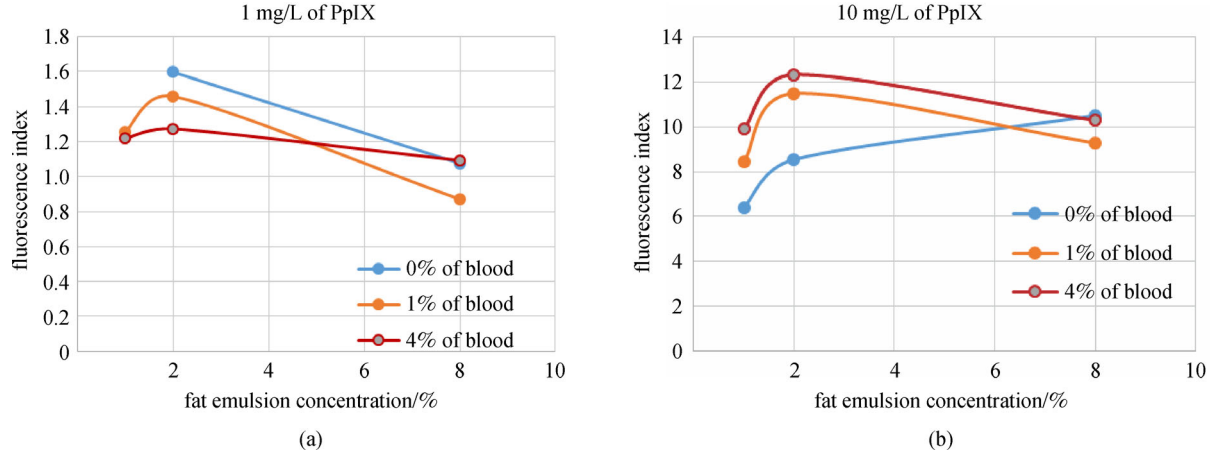


Fig. 5 Attenuation correction for fluorescence signal with linear approximation for (a) 1 mg/L of PpIX and (b) 10 mg/L of PpIX

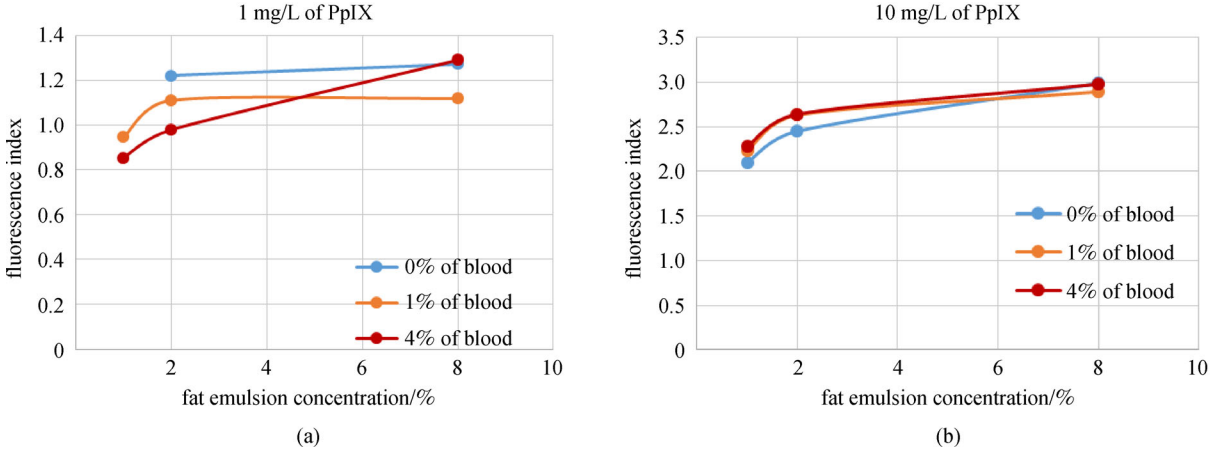


Fig. 6 Attenuation correction for fluorescence signal with the power law approximation for (a) 1 mg/L of PpIX and (b) 10 mg/L of PpIX

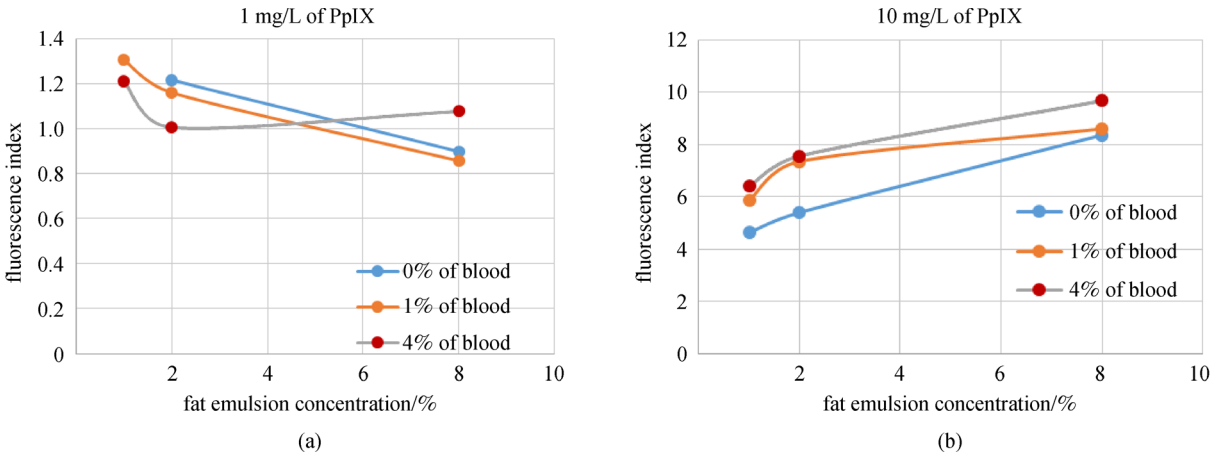


Fig. 7 Attenuation correction for fluorescence signal using the combined Beer–Lambert law approximation for (a) 1 mg/L of PpIX and (b) 10 mg/L of PpIX

Table 3 Results of fluorescence attenuation correction with different approximations

approximation type	average variation in determining the photosensitizer concentration for phantoms with 1 mg/L of PpIX/%	average variation in determining the photosensitizer concentration for phantoms with 10 mg/L of PpIX/%
fluorescence index	13	28
linear approximation	16	15
power-law approximation	11.6	9.6
combined (Lambert–Beer law and diffuse approximation)	14	18.5

change in scattering is considered to be the destruction of myelin. However, one cannot ignore the fact that tumors, as a rule, differ from normal tissues in terms of the degree of blood filling. Therefore, a comprehensive analysis of the influence of these factors on the recorded fluorescence signal is necessary to obtain reliable information on the concentration of the PS in tissues, especially in the area of infiltration of tumor cells into healthy tissues, where the accumulation of PS is small and the effect of absorption and scattering on the signal is especially critical for the sensitivity of the method.

4 Conclusions

In this study, a variant of the fiber-optic spectrometer with an extended dynamic range for the study of the content of fluorochromes in biological tissues with significantly different optical properties is proposed, which makes it possible to use it to study the PS distribution in the tissues and organs with significantly different optical properties. Various variants of approximation of the dependence of the fluorescence signal on the concentration of the scatterer and absorber for the correction of its attenuation in tissues are considered. The power law approximation is optimal for a given configuration of the fiber-optic sample, and it can be used to calculate the concentration of the PS at known concentrations of the scatterer and absorber with the least variation.

Acknowledgements The reported study was funded by Russian Foundation for Basic Research (RFBR) according to the research project No. 18-29-01062.

References

1. Loschenov V B, Linkov K G, Savelieva T A, Loschenov M V, Model S S, Borodkin A V. Hardware and tool equipment for fluorescence diagnostics and photodynamic therapy. Photodynamic Therapy and Photodyagnosis, 2013, 2(3): 17–25
2. Meerovich G A, Tiganova I G, Makarova E A, Meerovich I G, Romanova J, Tolordova E R, Alekseeva N V, Stepanova T V, Yu K, Lukyanets E A, Krivospitskaya N V, Sipailo I P, Baikova T V, Loschenov V B, Gonchukov S A. Photodynamic inactivation of bacteria and biofilms using cationic bacteriochlorins. Journal of Physics: Conference Series, 2016, 691: 012011
3. Meerovich G A, Akhlyustina E V, Tiganova I G, Panov V A, Tyukova V S, Tolordava E R, Alekseeva N V, Linkov K G, Romanova Yu M, Grin M A, Mironov A F, Loshchenov V B, Kaprin A D, Filonenko E V. Study of photosensitizer for antibacterial photodynamic therapy based on cyclodextrin formulation of 13^3-n-(n-methylnicotinyl)bacteriopurpurinimide methyl

ester. Biomedical Photonics, 2017, 6(3): 16–32
4. Bradley R S, Thorniley M S. A review of attenuation correction techniques for tissue fluorescence. Journal of the Royal Society, Interface, 2006, 3(6): 1–13
5. Haj-Hosseini N, Lowndes S, Salerud G, Wårdell K. Blood interference in fiber-optical based fluorescence guided resection of glioma using 5-aminolevulinic acid. In: Proceedings of SPIE 7883, Photonic Therapeutics and Diagnostics. San Francisco: SPIE, 2011, VII: 78833R
6. Zhang Y, Hou H, Zhang Y, Wang Y, Zhu L, Dong M, Liu Y. Tissue intrinsic fluorescence recovering by an empirical approach based on the PSO algorithm and its application in type 2 diabetes screening. Biomedical Optics Express, 2018, 9(4): 1795–1808
7. Jöbsis F F, O'Connor M, Vitale A, Vreman H. Intracellular redox changes in functioning cerebral cortex. I. Metabolic effects of epileptiform activity. Journal of Neurophysiology, 1971, 34(5): 735–749
8. Kramer R S, Pearlstein R D. Cerebral cortical microfluorometry at isosbestic wavelengths for correction of vascular artifact. Science, 1979, 205(4407): 693–696
9. Canpolat M, Mourant J R. Optical measurement of photosensitizer concentration using a probe with a small source-detector fiber separation. Proceedings of the Society for Photo-Instrumentation Engineers, 2000, 3911: 10–18
10. Meerovich G A, Akhlyustina E V, Savelieva T A, Linkov K G, Loschenov V B. Optical spectroanalyzer with extended dynamic range for pharmacokinetic investigations of photosensitizers in biotissue. Biomedical Photonics, 2019, 8(1): 46–51
11. Studinski R C, Vitkin I A. Methodology for examining polarized light interactions with tissues and tissuelike media in the exact backscattering direction. Journal of Biomedical Optics, 2000, 5(3): 330–337
12. Kalyagina N, Loschenov V, Wolf D, Daul C, Blondel W, Savelieva T. Experimental and Monte Carlo investigation of visible diffuse-reflectance imaging sensitivity to diffusing particle size changes in an optical model of a bladder wall. Applied Physics B, Lasers and Optics, 2011, 105(3): 631–639
13. Kalkman J, Bykov A V, Faber D J, van Leeuwen T G. Multiple and dependent scattering effects in Doppler optical coherence tomography. Optics Express, 2010, 18(4): 3883–3892
14. Martelli F, Zaccanti G. Calibration of scattering and absorption properties of a liquid diffusive medium at NIR wavelengths. CW method. Optics Express, 2007, 15(2): 486–500
15. Di Ninni P, Martelli F, Zaccanti G. Effect of dependent scattering on the optical properties of Intralipid tissue phantoms. Biomedical Optics Express, 2011, 2(8): 2265–2278
16. Michels R, Foschum F, Kienle A. Optical properties of fat emulsions. Optics Express, 2008, 16(8): 5907–5925
17. Prahl S. Optical absorption of hemoglobin. Available at omlc.org/spectra/hemoglobin/
18. Delpy D T, Cope M, van der Zee P, Arridge S, Wray S, Wyatt J. Estimation of optical pathlength through tissue from direct time of flight measurement. Physics in Medicine and Biology, 1988, 33(12): 1433–1442
19. Savelieva T A, Loshchenov V B, Goryainov S A, Shishkina L V, Potapov A A. A spectroscopic method for simultaneous determination of protoporphyrin IX and hemoglobin in the nerve tissues at intraoperative diagnosis. Russian Journal of General Chemistry, 2015, 85(6): 1549–1557
20. Goryaynov S A, Okhlopkov V A, Golbin D A, Chernyshov K A, Svistov D V, Martynov B V, Kim A V, Byvaltsev V A, Pavlova G V, Batalov A, Konovalov N A, Zelenkov P V, Loschenov V B, Potapov A A. Fluorescence diagnosis in neurooncology: retrospective analysis of 653 cases. Frontiers in Oncology, 2019, 9: 830



Tatiana A. Savelieva received her Master of Engineering degree with a specialization in Engineering in biomedical practice in 2005 and Ph.D. degree in Laser Physics in 2013 from A.M. Prokhorov General Physics Institute of the Russian Academy of Sciences, Russia.

Now Tatiana A. Savelieva is working as a researcher at General Physics Institute and an associate professor at National Research Nuclear University MEPhI, Russia. The area of scientific interests includes biophotonics and various methods of optical spectroscopy applied to the differentiation of biological tissues.



Marina N. Kuryanova received her Master's degree in Nuclear Physics and Technology from National Research Nuclear University MEPhI, Russia. She completed her pre-graduate practice at Department of Laser, Micro and Nanosystems. Recently, she was engaged in solving the problem of improving the accuracy of fluorescence diagnostics in conditions of significantly different optical properties of the studied organs and tissues. Solving this problem will increase the effectiveness of diagnostics and determining the boundaries of tumors.



Ekaterina V. Akhlyustina studied at National Research Nuclear University MEPhI, Russia, in 2011–2015 at the department No. 35 "Medical Physics", the direction of training "Radiation Biophysics", a diploma was written on the topic "The effect of different doses of gamma radiation on neurogenesis in the dentate fascia of the hippocampus and on the spatial behavior of adult mice" (head Lazutkin A.A.). In 2015–2017, she studied at National Research Nuclear University MEPhI at the department No. 87 "Laser micro-, nano- and biotechnologies", the direction of training was "Biomedical Photonics". From 2017 to present time, she is postgraduate student at National Research Nuclear University MEPhI, direction of training "Physics and Astronomy".



Kirill G. Linkov received his Master of Engineering degree with a specialization in Electronic Devices and Equipment (Electronics and optoelectronic engineering dept.) in 1994 and Ph.D. degree in Engineering with a specialization in Quantum Electronics in 1999 from Moscow Institute of Radio Engineering, Electronics and Automation, Russia.

Kirill G. Linkov is Senior Scientist at Prokhorov General Physics Institute of the Russian Academy of Sciences, Russia, and engages in development of methods for laser-fluorescent diagnostics, and photodynamic therapy. He takes part as Investigator or Principal Investigator in the research projects that are being implemented with financial support from Russian Foundation for Basic Research (RFBR), Russian State Atomic Energy Corporation "Rosatom", Ministry of Education and Science of the Russian Federation, Russia. Kirill G. Linkov has presented in various professional conferences and has more than 40 published works including publications in peer-reviewed journals, such as *Laser Physics*, *Lasers in Medical Science*, *Methods and Applications in Fluorescence*, *Biomedical Photonics*. He is also the author or co-author of more than 20 patents.



Gennady A. Meerovich is Senior Scientist at Prokhorov General Physics Institute of the Russian Academy of Sciences, associate professor at National Research Nuclear University MEPhI, Russia. He received the degree of "Candidate of Physical and Mathematical Sciences", eq. to the international Ph.D. degree, in 1981 with topic of PhD Thesis: "Investigation and optimization of active elements of scanning Semiconductor Electron-Beam-Pumped Lasers". From 1994 till present, he is working as senior researcher in Laser Biospectroscopy Laboratory (Center for Nature Science Investigations, General Physics Institute of the Russian Academy of Sciences, Moscow, Russia) on research and development of new methods, devices and photosensitizers for photodynamic treatment and fluorescent diagnostics of cancer. Novel lasers and laser systems, scanning laser systems, computer-assisted system for diagnostics are also in the field of his scientific interests.



Victor B. Loschenov is professor and head of laboratory at Prokhorov General Physics Institute of the Russian Academy of Sciences, professor at National Research Nuclear University (NRNU) MEPhI, Russia. His research interests are focused on fundamentals and practical applications of photodynamic therapy and fluorescent diagnostics of cancer, medical devices, phototheranostics, different modalities of optical spectroscopy. He received the Ph.D. degree in 1981 from N.S. Kurnakov Institute of General and Inorganic Chemistry, Academy of Sciences of the USSR on specialty "Quantum radio physics". In 2006, he received the degree of doctor of science in laser physics from Prokhorov General Physics Institute of the Russian Academy of Sciences with subject: "Methods and apparatus for spectral-fluorescence diagnosis and photodynamic therapy". Since 2007, he has a title of professor in Laser physics. His professional experience includes the position of head of Laser Biospectroscopy Laboratory at GPI RAS (Moscow, Russia) (from 1989 till present) and professor and head of department in NRNU MEPHI, Russia.